Space group symmetry, spin-orbit coupling and the low energy effective Hamiltonian for iron based superconductors

Phys. Rev. B **88**, 134510 (2013)

Oskar Vafek

National High Magnetic Field Laboratory

and

Florida State University

Tallahassee, FL

KITP, Sep 9, 2014

Collaborators

Dr. Vladimir Cvetkovic (NHMFL, FSU)

NSF Career award: Grant No. DMR-0955561,
NSF Cooperative Agreement No. DMR-0654118, and the State of Florida

National High Magnetic Field Laboratory
Florida State University

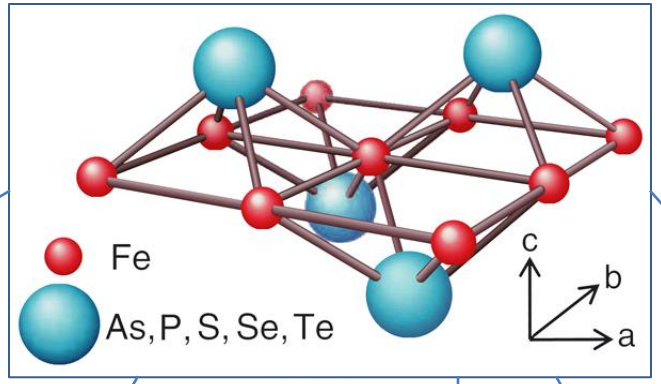

Common structural unit is the 2D Fe plane

42622
(32522)

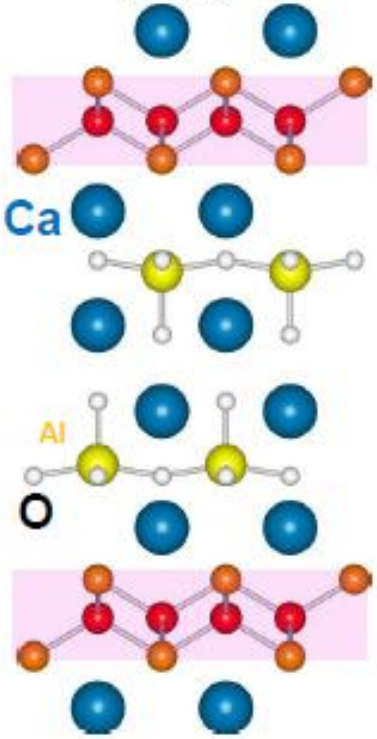

$(A_4M_2O_6)\ Fe_2As_2$

T_c(max)=47K

Zhu et al.(2009)
Ogino et al. (2009)

1111

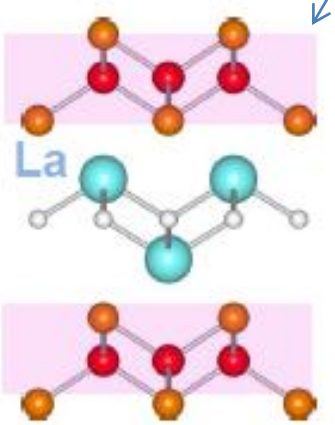

Ln FeAsO

T_c(max)=55K

Y. Kamihara et al.(2008)

122

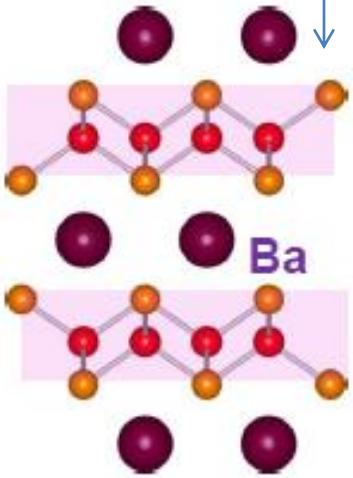

$BaFe_2As_2$

T_c(max)=38K

M. Rotter et al.(2008)

111

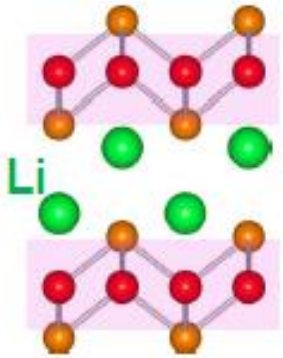

LiFeAs

T_c= 18 K

X.C.Wang et al.(2008)

11

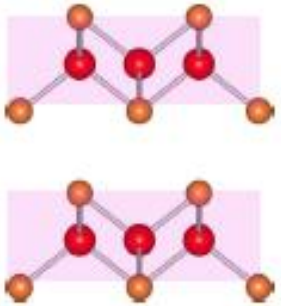

FeSe

T_c= 8 K

F.C.Hsu et al.(2008)

Yuji Matsuda, Lectures NSF Boulder Summer School 2014

$La^{3+}Fe^{2+}As^{3-}O^{2-}$ => six electrons on iron (at stoichiometry)

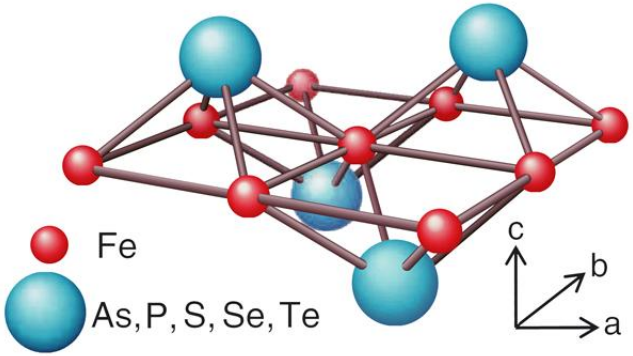

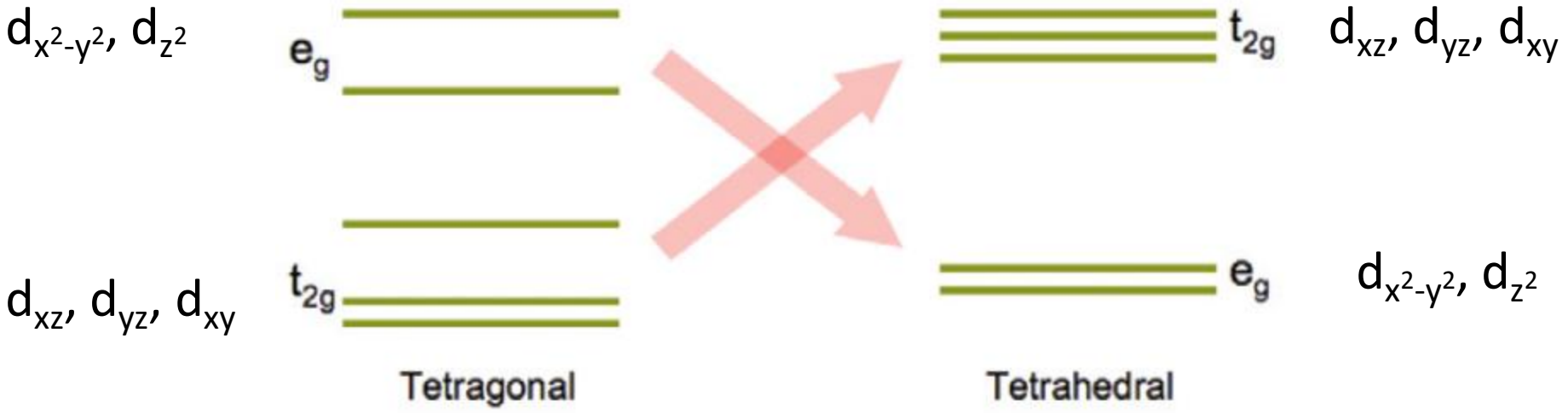

From: Cvetkovic and Tesanovic, EPL **85,** 37002 (2009).

$La^{3+}Fe^{2+}As^{3-}O^{2-}$ => six electrons on iron (at stoichiometry)

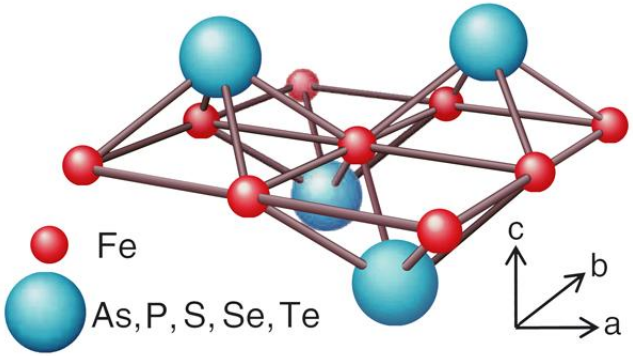

2 iron atoms/unit cell

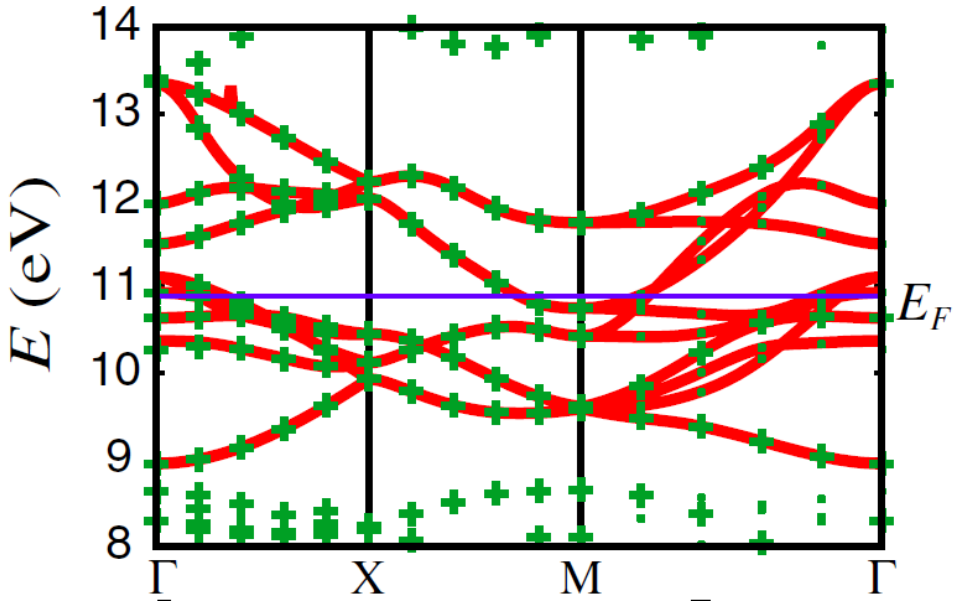

Strong hybridization of all five d-orbitals

From: Kuroki *et.al.*, PRL **101,** 087004 (2008).

- Fe 3d electrons are at the Fermi level (take part in sc)
- In most (but not all) *Fe*SC, iron 3d electrons are magnetic.
  Counter examples are e.g. *LiFeAs* and *FeSe*
- For undoped 1111 and 122, there are both SDW and structural transitions
  Neither spin density wave nor structural trans. in *LiFeAs* but both in *NaFeAs*.
  Also, sc *FeSe* shows structural trans. but no magnetic trans.
  $Fe_{1-y}Se_xTe_{1-x}$ for x>0.05 has both struct. and magnetic trans.

Spin Density Wave:

1111 and 122
(parent compound metallic, 0.36-0.87μ_B/Fe)

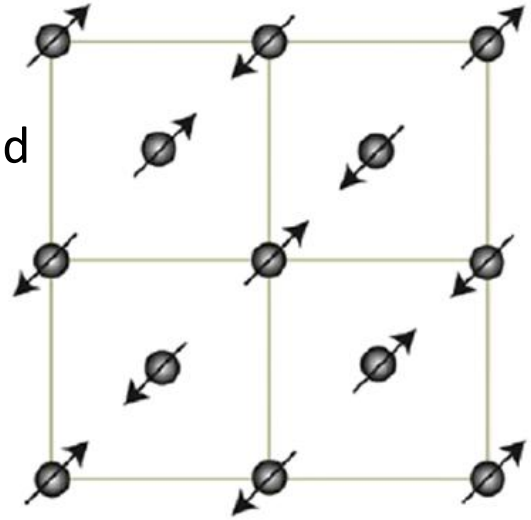

FeTe
(conducting but ρ~ mΩcm 2.25μ_B/Fe)

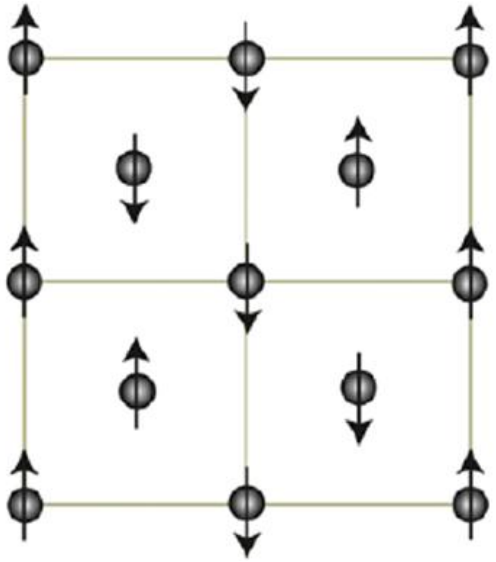

From: G.R. Stewart Rev. Mod. Phys. 2011

Low carrier density, quasi 2D system
parent state is a compensated semi-metal.

Ultimate goal is to develop a microscopic theory of the various instabilities (not this talk)

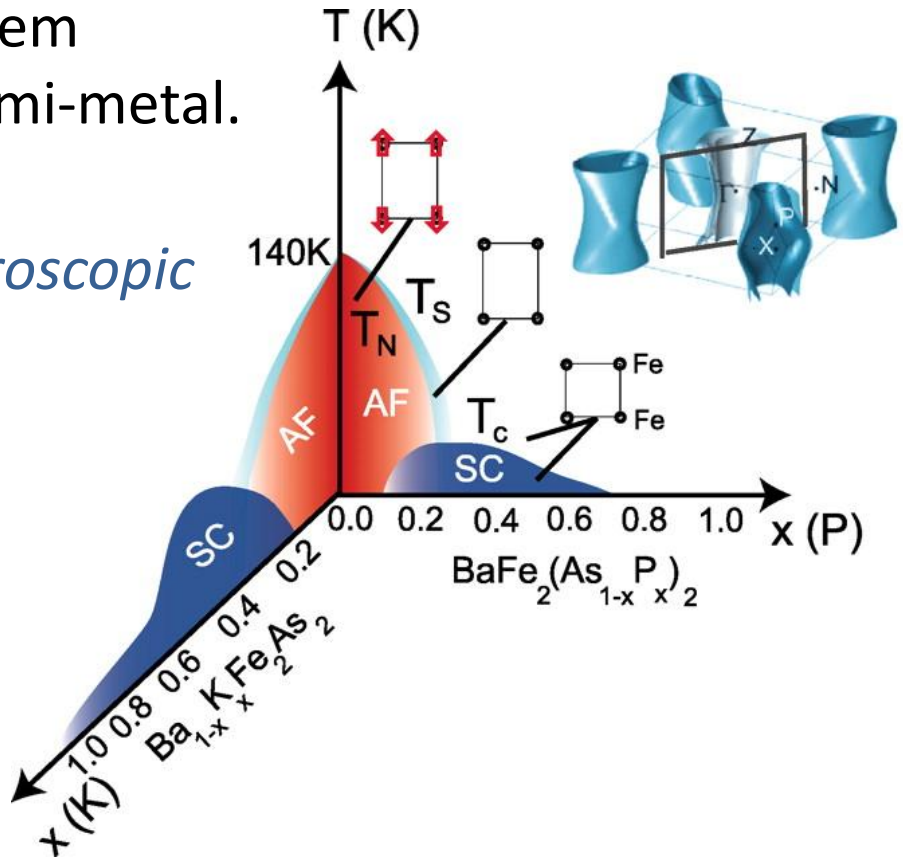

Our main results

- Construction of the minimal low energy continuum model based on the space group symmetry (including spin-orbit interaction)

- Order parameters classified using the representations of space group
  - collinear SDW –Kramers degeneracy present
  - coplanar SDW –Kramers degeneracy absent
  - spin-orbit: spin direction locking and induced pnictogen magnetic moment

- A_{1g}-superconductivity (s-wave) without spin-orbit:
  - spin-singlet: 3 parameters; gap isotropic at Γ, anisotropic at **M**

- A_{1g}-superconductivity (s-wave) with spin-orbit:
  - spin-triplet admixture; 2 parameters; anisotropy and near nodes at Γ, 4-fold gap dependence at M

Lattice structure of iron-pnictides

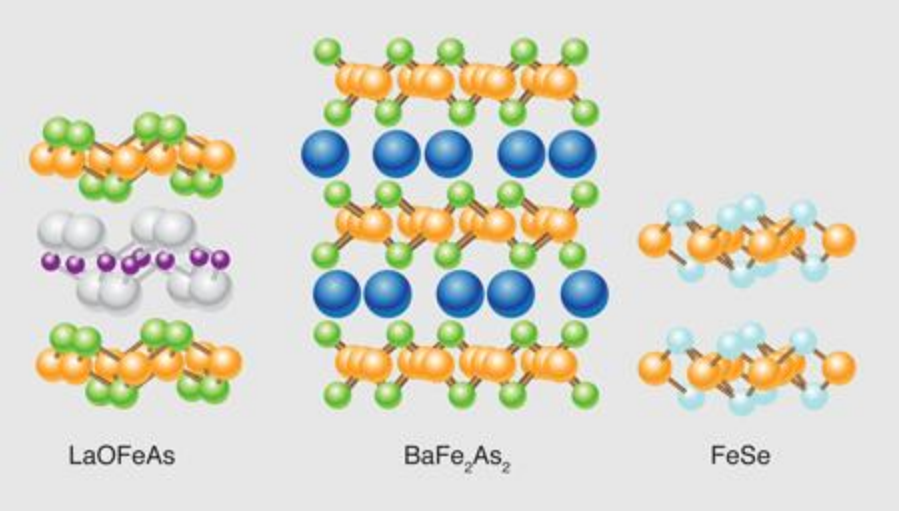

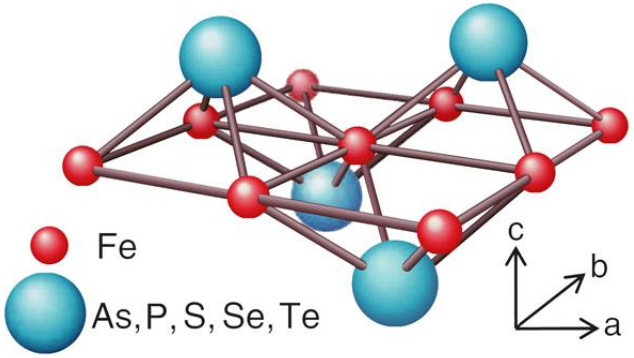

Pnictide families:

1111: REOFeAs, LaOFeP, REFFeAs
122: BaFeAs
11: FeTe, FeSe
111: LiFeAs
…

Space group:

1111: P4/nmm (129)
122: I4/mmm (139)
11: P4/nmm (129)
111: P4/nmm (129)

Space group *P4/nmm*: **non-symmorphic**

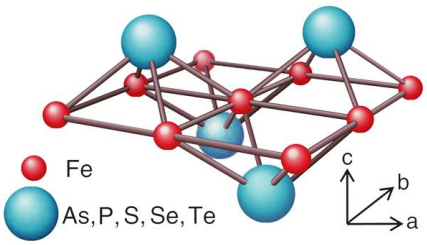

Generators:

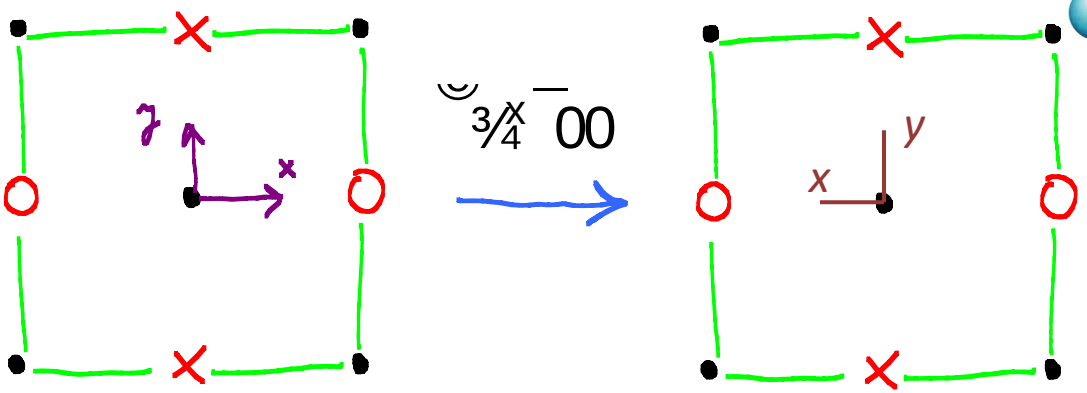

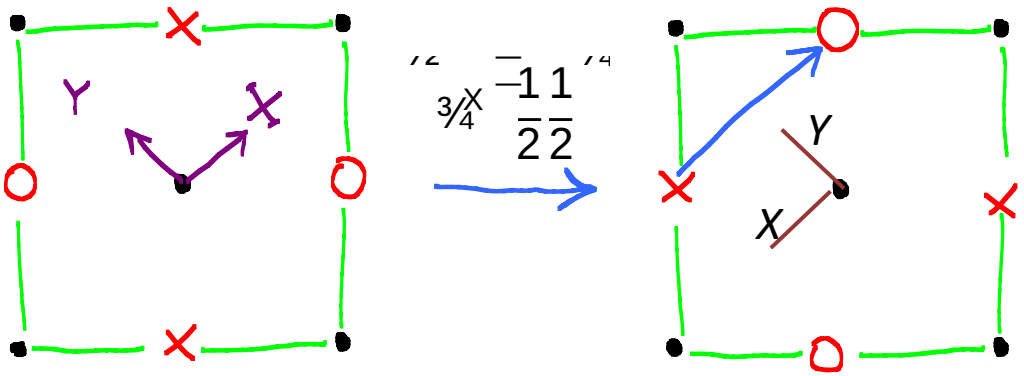

n-glide plane

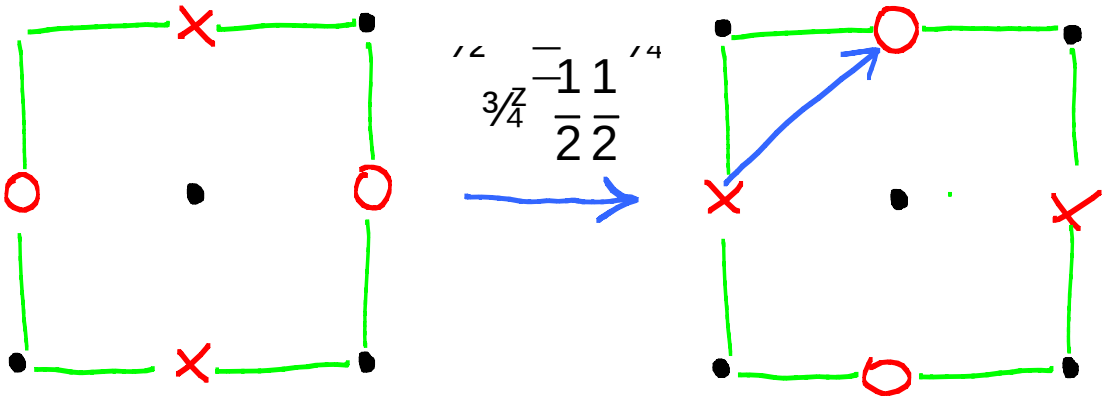

Irreducible representations of the space group

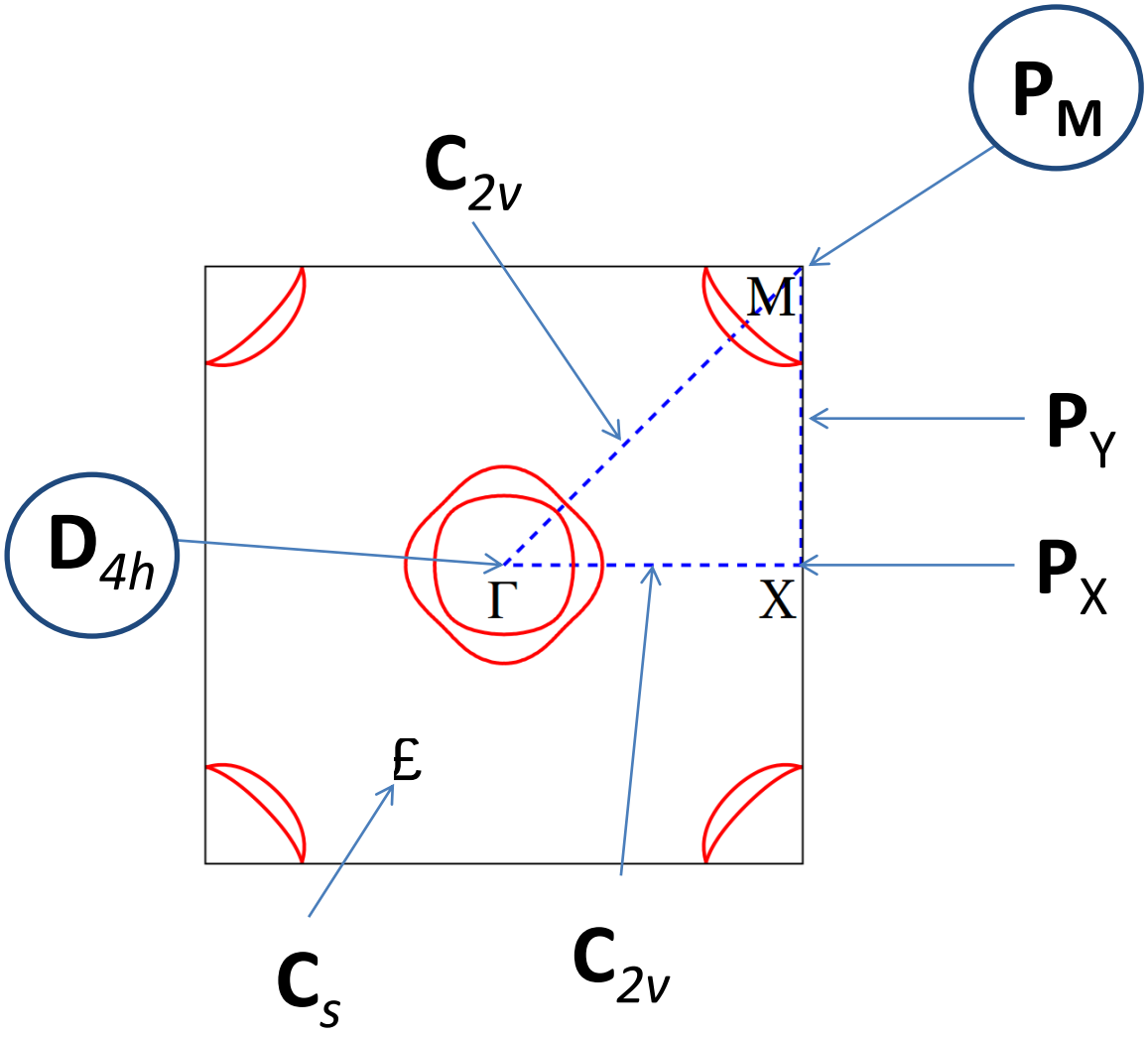

Irreducible representations of the space group at the **M**-point

At **M**-point: $\mathbf{D}_{4h}$ is not closed due to fractional translations, e.g.

$$\left\{\sigma^{X}\left|\tfrac{1}{2}\tfrac{1}{2}\right.\right\}\left\{\sigma^{X}\left|\tfrac{1}{2}\tfrac{1}{2}\right.\right\}=\left\{e\left|11\right.\right\}$$

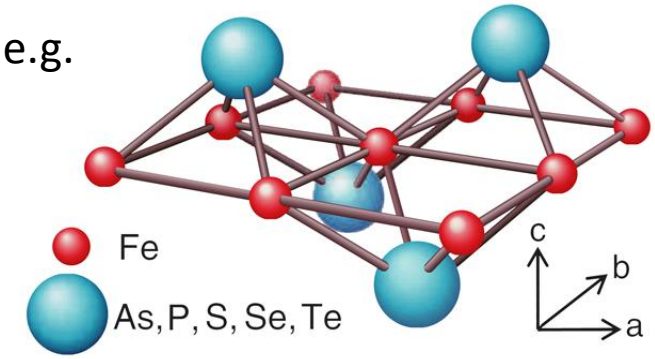

The group of the wave-vector, $\mathbf{P}_{\mathbf{M}}$, is a factor group of P4/nmm w.r.t. ``even'' translations (C. Herring, 1942)

32 elements (16 from $\mathbf{D}_{4h}$ and 16 with an odd translation added)

Only 2D irreducible representations are physical!

$\mathbf{P_M}$	$\{\sigma^X\|\frac{1}{2}\frac{1}{2}\}$	$\{\sigma^z\|\frac{1}{2}\frac{1}{2}\}$	$\{\sigma^x\|00\}$
E_{M1}	$\begin{bmatrix}-1 & 0\\ 0 & -1\end{bmatrix}$	$\begin{bmatrix}-1 & 0\\ 0 & 1\end{bmatrix}$	$\begin{bmatrix}0 & 1\\ 1 & 0\end{bmatrix}$
E_{M2}	$\begin{bmatrix}1 & 0\\ 0 & 1\end{bmatrix}$	$\begin{bmatrix}-1 & 0\\ 0 & 1\end{bmatrix}$	$\begin{bmatrix}0 & 1\\ 1 & 0\end{bmatrix}$
E_{M3}	$\begin{bmatrix}1 & 0\\ 0 & -1\end{bmatrix}$	$\begin{bmatrix}-1 & 0\\ 0 & 1\end{bmatrix}$	$\begin{bmatrix}0 & 1\\ 1 & 0\end{bmatrix}$
E_{M4}	$\begin{bmatrix}-1 & 0\\ 0 & 1\end{bmatrix}$	$\begin{bmatrix}-1 & 0\\ 0 & 1\end{bmatrix}$	$\begin{bmatrix}0 & 1\\ 1 & 0\end{bmatrix}$

Symmetry adapted functions at **M**-point

The lowest harmonics

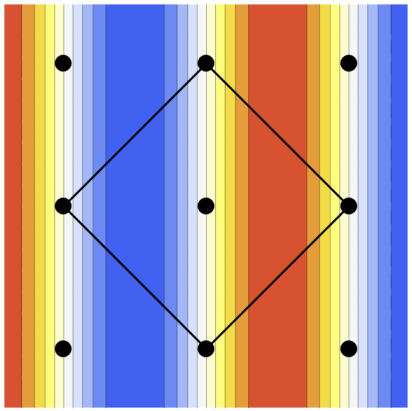

$E_{\mathbf{M}2}{}^{X}$

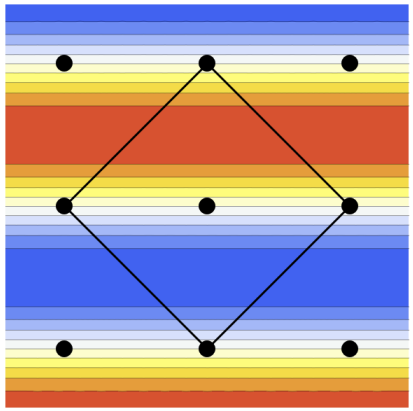

$E_{\mathbf{M}2}{}^{Y}$

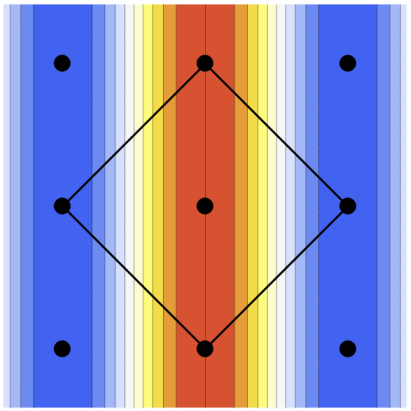

$E_{\mathbf{M}4}{}^{X}$

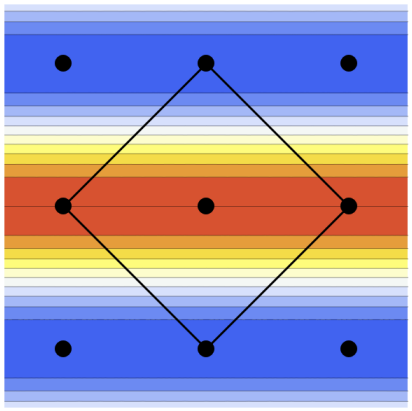

$E_{\mathbf{M}4}{}^{Y}$

Next harmonics

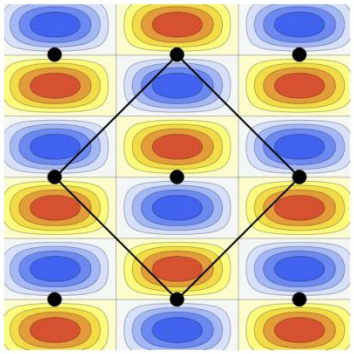

$E_{\mathbf{M}1}{}^{X}$

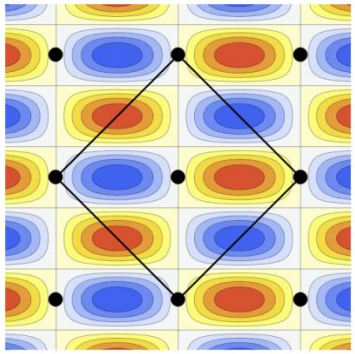

$E_{\mathbf{M}2}{}^{X}$

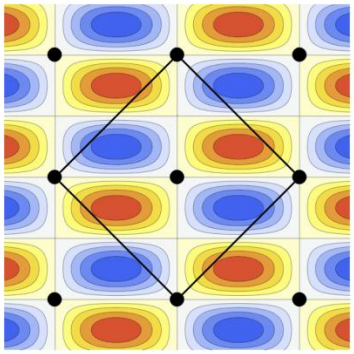

$E_{\mathbf{M}3}{}^{X}$

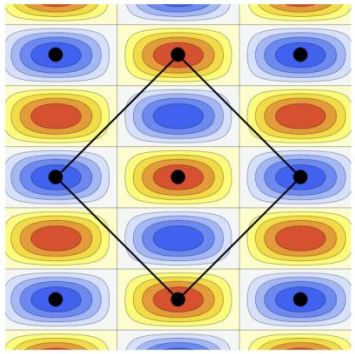

$E_{\mathbf{M}4}{}^{X}$

Full tight banding band structure

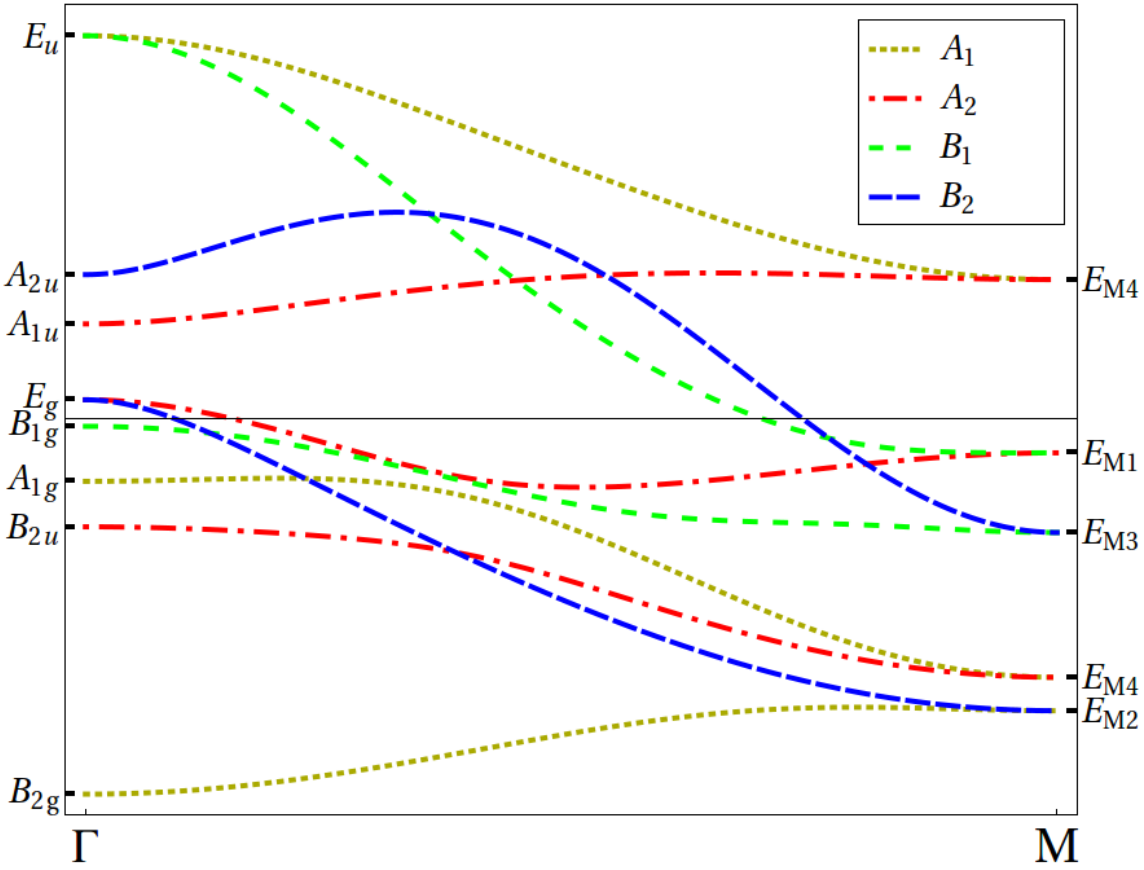

K. Kuroki, *et al*., Phys. Rev. Lett. **101**, 087004 (2008)

Fermi surface states' symmetries:

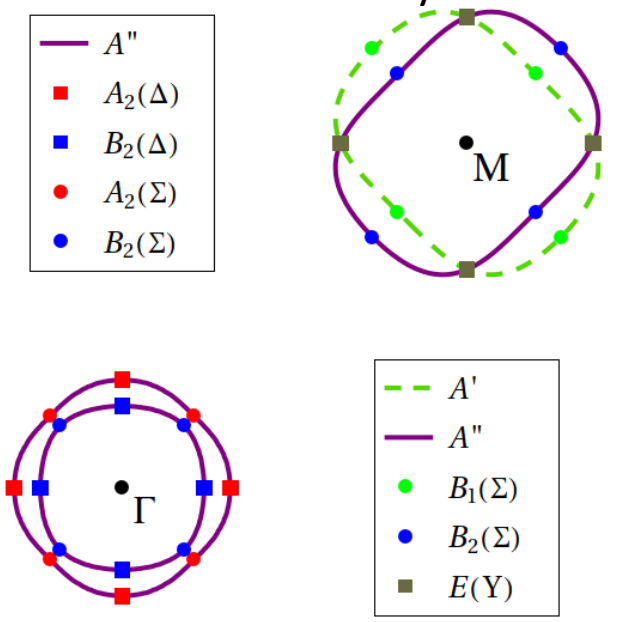

Full tight banding band structure and the low energy spinor

$$\psi_\sigma(\mathbf{k}) = \begin{pmatrix} \psi_{X,\sigma}(\mathbf{k}) \\ \psi_{Y,\sigma}(\mathbf{k}) \\ \psi_{\Gamma,\sigma}(\mathbf{k}) \end{pmatrix}$$

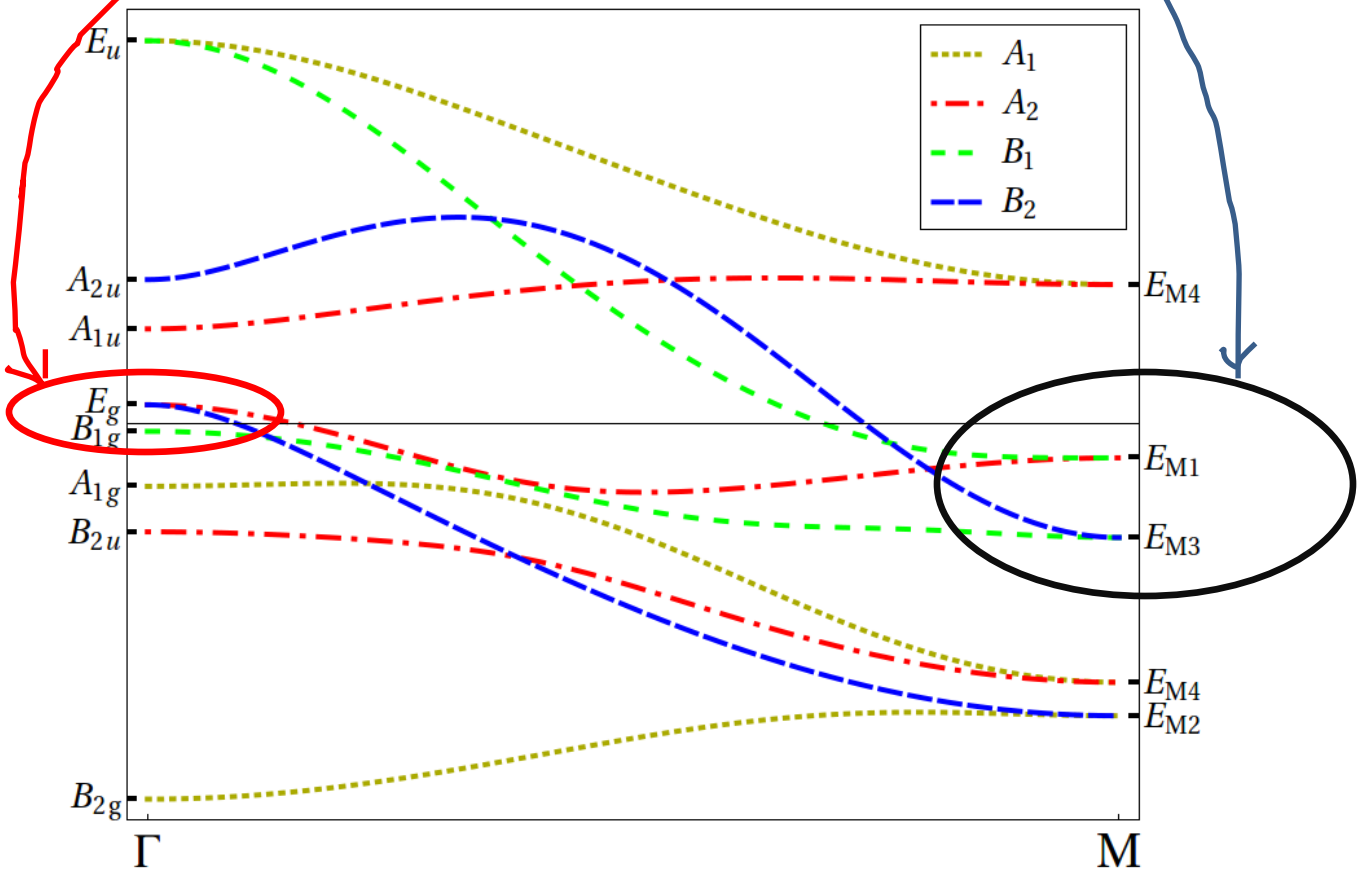

Low-energy effective theory

Low-energy spinor
(Γ: E_g states; **M**: E_{M1} and E_{M3} states):

$$\psi_\sigma(\mathbf{k}) = \begin{pmatrix} \psi_{X,\sigma}(\mathbf{k}) \\ \psi_{Y,\sigma}(\mathbf{k}) \\ \psi_{\Gamma,\sigma}(\mathbf{k}) \end{pmatrix}$$

Yz_A+Yz_B
$-Xz_A-Xz_B$

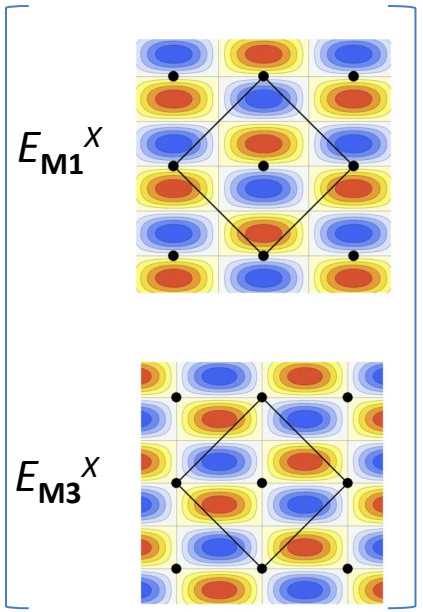

ODD under n-glide

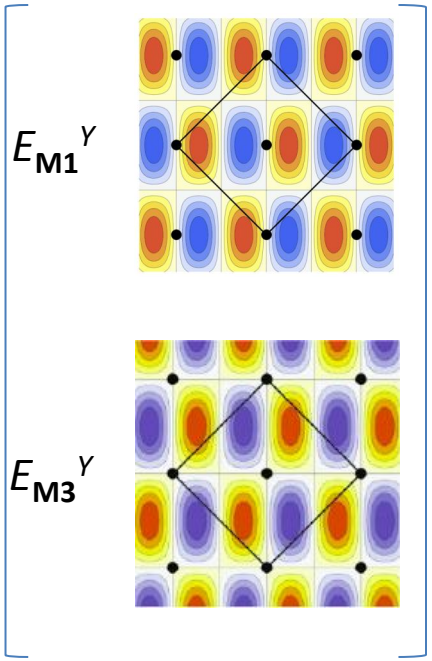

EVEN under n-glide

=> Do not mix (at k_z=0)

Low-energy effective theory

Low-energy spinor (Γ: E_g states; **M**: E_{M1} and E_{M3} states):

$$\psi_\sigma(\mathbf{k}) = \begin{pmatrix} \psi_{X,\sigma}(\mathbf{k}) \\ \psi_{Y,\sigma}(\mathbf{k}) \\ \psi_{\Gamma,\sigma}(\mathbf{k}) \end{pmatrix}$$

$$H_0 = \sum_{\mathbf{k},\sigma=\uparrow,\downarrow} \psi_\sigma^\dagger(\mathbf{k}) \begin{pmatrix} h_{\mathbf{M}}^+(\mathbf{k}) & 0 & 0 \\ 0 & h_{\mathbf{M}}^-(\mathbf{k}) & 0 \\ 0 & 0 & h_\Gamma(\mathbf{k}) \end{pmatrix} \psi_\sigma(\mathbf{k})$$

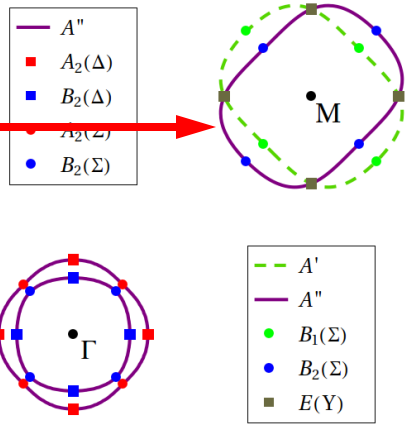

Low-energy effective theory

$$H_0 = \sum_{\mathbf{k},\sigma=\uparrow,\downarrow} \psi^\dagger_\sigma(\mathbf{k}) \begin{pmatrix} h^+_{\mathbf{M}}(\mathbf{k}) & 0 & 0 \\ 0 & h^-_{\mathbf{M}}(\mathbf{k}) & 0 \\ 0 & 0 & h_\Gamma(\mathbf{k}) \end{pmatrix} \psi_\sigma(\mathbf{k})$$

The individual blocks:

$$h^\pm_{\mathbf{M}}(\mathbf{k}) = \begin{pmatrix} \varepsilon_1 + \frac{\mathbf{k}^2}{2m_1} \pm a_1 k_x k_y & -iv_\pm(\mathbf{k}) \\ iv_\pm(\mathbf{k}) & \varepsilon_3 + \frac{\mathbf{k}^2}{2m_3} \pm a_3 k_x k_y \end{pmatrix}$$

$$h_\Gamma(\mathbf{k}) = \begin{pmatrix} \varepsilon_\Gamma + \frac{\mathbf{k}^2}{2m_\Gamma} + b k_x k_y & c\left(k_x^2 - k_y^2\right) \\ c\left(k_x^2 - k_y^2\right) & \varepsilon_\Gamma + \frac{\mathbf{k}^2}{2m_\Gamma} - b k_x k_y \end{pmatrix}$$

Fitting to the full models for iron-pnictides

	ε_Γ	ε_1	ε_3	$1/(2m_\Gamma)$	$1/(2m_1)$	$1/(2m_3)$	a_1	a_3	b	c	v	p_1	p_2
EPL **85**, 37002 (2009)	132	−400	−647	−184	149	317	419	−533	56.5	−62.3	−243	−40	10
PRL **101**, 087004 (2008)	100	−180	−600	−462	−65.9	322	41.8	−384	438	244	99.0	39.1	0.99

Comparison of the low-energy effective theory to the full models

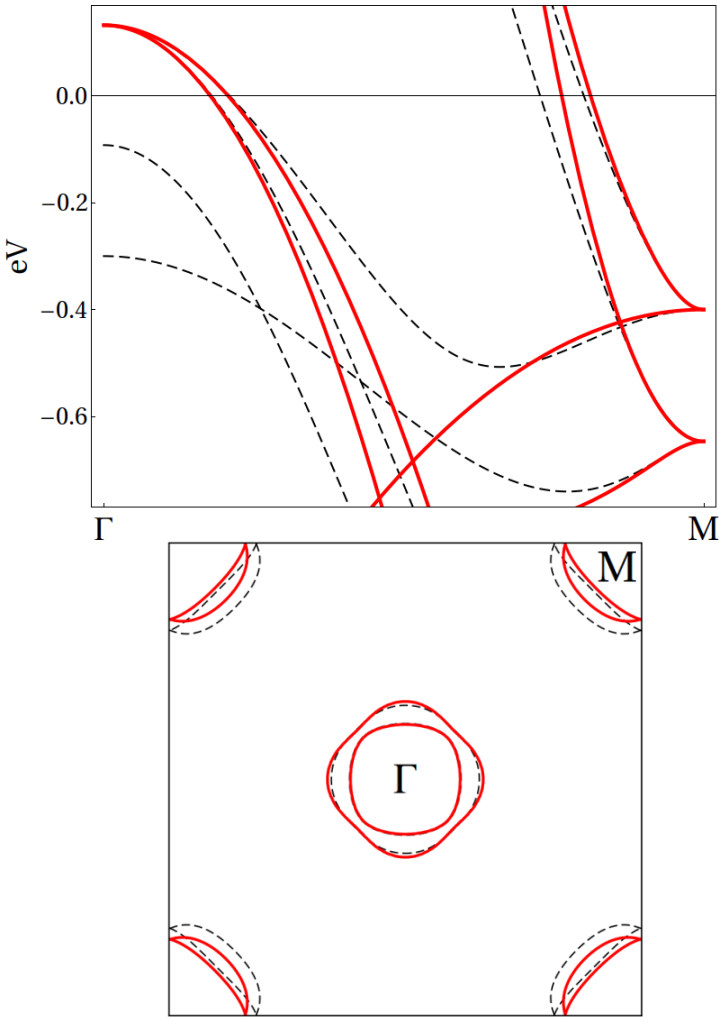

V. Cvetkovic, Z. Tesanovic, Europhys. Lett. **85**, 37005 (2009)

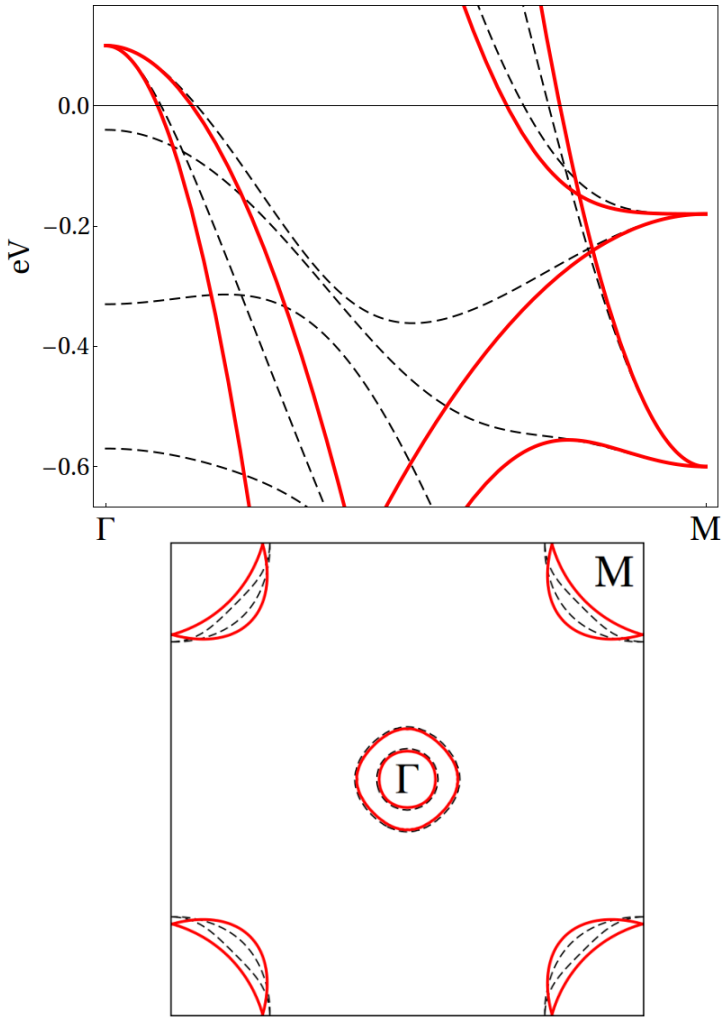

K. Kuroki, *et al.*, Phys. Rev. Lett. **101**, 087004 (2008)

Comparison of the low energy effective theory to 2-orbital models

Only d_{xz} and d_{yz} iron orbitals:
- at Γ: E_g and E_u states
- at **M**: $E_{\mathbf{M1}}$ and $E_{\mathbf{M2}}$ states

S. Raghu, et al., Phys. Rev. B **77**, 220503R (2008)

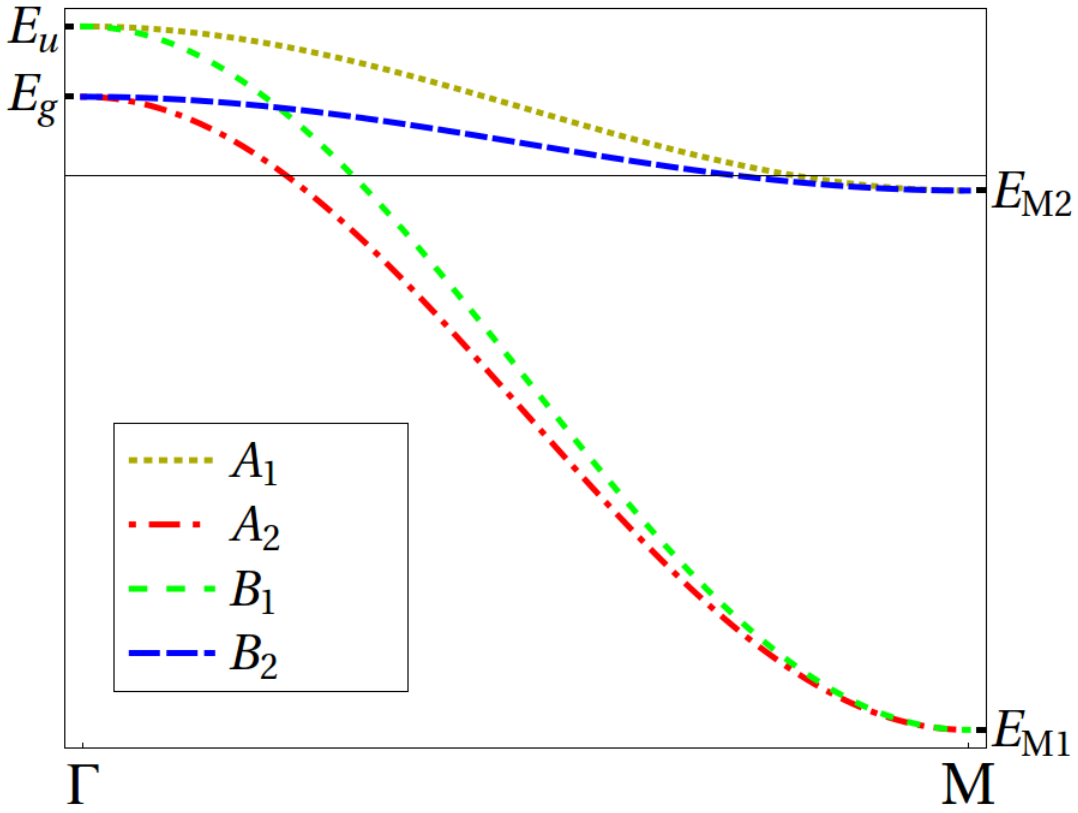

Violates mirror symmetries through Fe-As bonds:

J. Hu and N. Hao, Phys. Rev. X **2**, 021009 (2012)

Comparison of the low energy effective theory to 3-orbital models

Only d_{xz}, d_{yz}, and d_{XY} iron orbitals

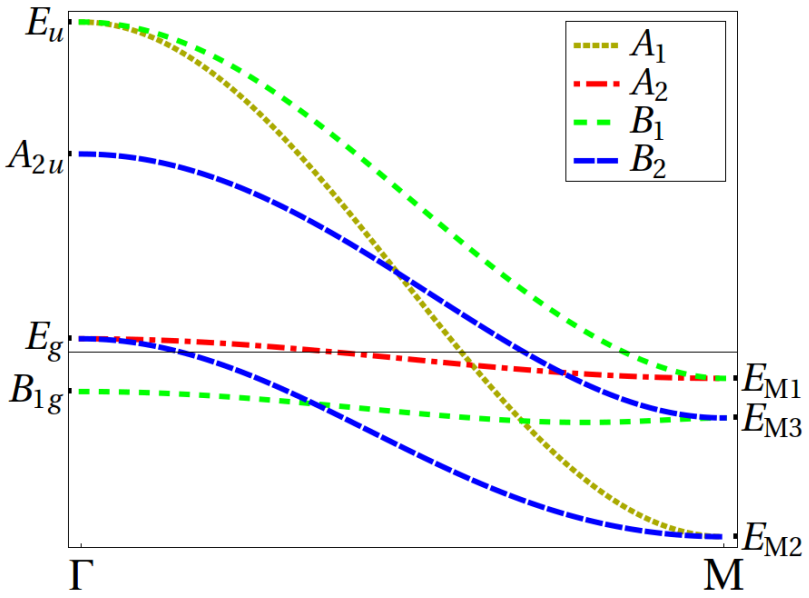

P. A. Lee and X.-G. Wen, Phys. Rev. B **78**, 144517 (2008)

- at Γ and **M**: correct symmetry properties of the bands
- spurious Fermi surface

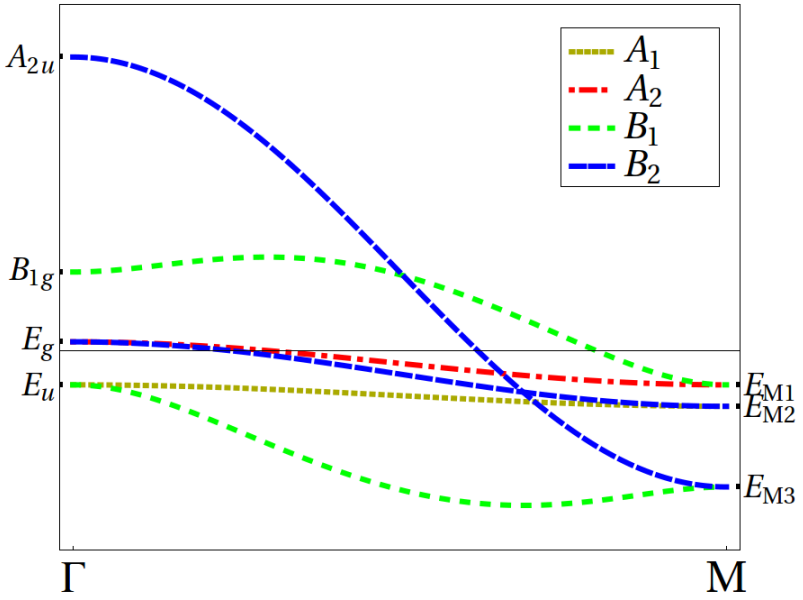

M. Daghofer, et al., Phys. Rev. B **81**, 014511 (2010)

- no spurious Fermi surfaces
- at Γ and **M** wrong band ordering

Spin-orbit interaction in the low-energy effective theory

On-site spin-orbit interaction for iron 3d orbitals comparable to other energy scales

λ = 80meV (Fe clusters) M. L. Tiago, *et al*., Phys. Rev. Lett. **97**, 147201 (2006).

λ = 70meV (bcc Fe) Y. Yao, *et al*., Phys. Rev. Lett. **92**, 037204 (2004).

$$H_{so} = \sum_{\mathbf{k}} \sum_{\sigma,\sigma'} \psi^{\dagger}_{\sigma}(\mathbf{k}) \begin{pmatrix} 0 & h^{so}_{\mathbf{M},\sigma\sigma'} & 0 \\ \left(h^{so\,\dagger}_{\mathbf{M}}\right)_{\sigma\sigma'} & 0 & 0 \\ 0 & 0 & h^{so}_{\Gamma,\sigma\sigma'} \end{pmatrix} \psi_{\sigma'}(\mathbf{k})$$

$$h^{so}_{\Gamma,\sigma\sigma'} = \frac{1}{2}\lambda_{\Gamma} \begin{pmatrix} 0 & -i \\ i & 0 \end{pmatrix} \sigma^{3}_{\sigma\sigma'}$$

$$h^{so}_{\mathbf{M},\sigma\sigma'} = \frac{i}{2}\lambda_{\mathbf{M}} \left[\begin{pmatrix} 0 & 1 \\ 0 & 0 \end{pmatrix} \sigma^{1}_{\sigma\sigma'} + \begin{pmatrix} 0 & 0 \\ 1 & 0 \end{pmatrix} \sigma^{2}_{\sigma\sigma'} \right]$$

h^{so}_{Γ} Kane-Mele like term

Spin-orbit interaction in the low-energy effective theory

The effect on the spectrum

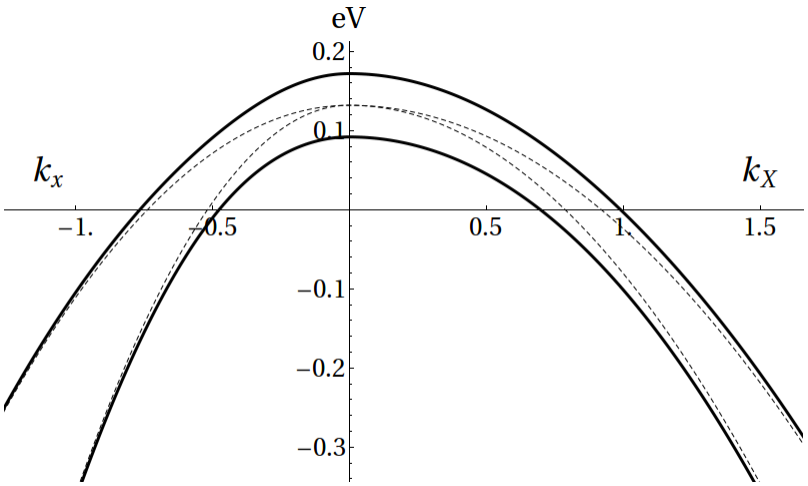

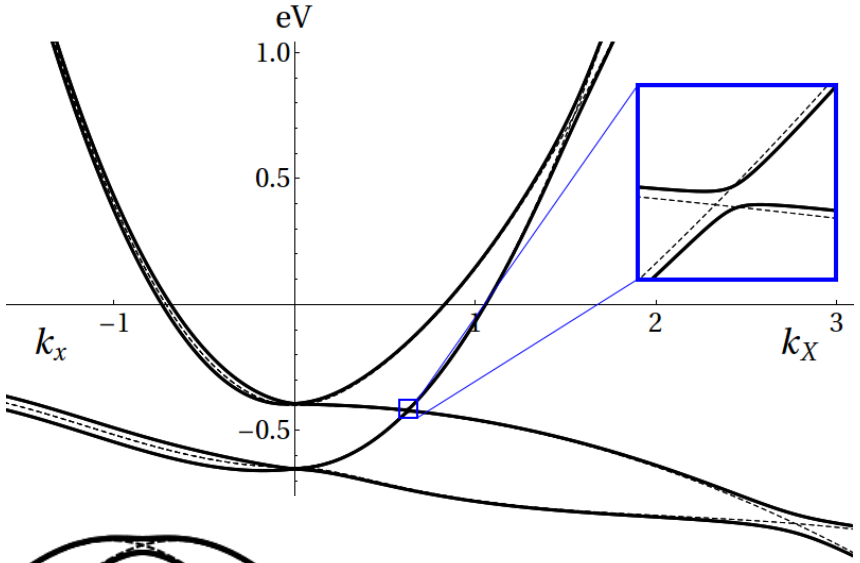

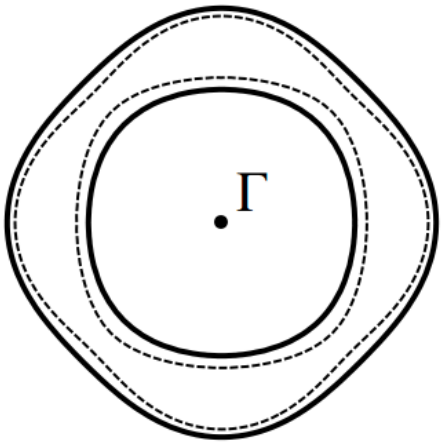

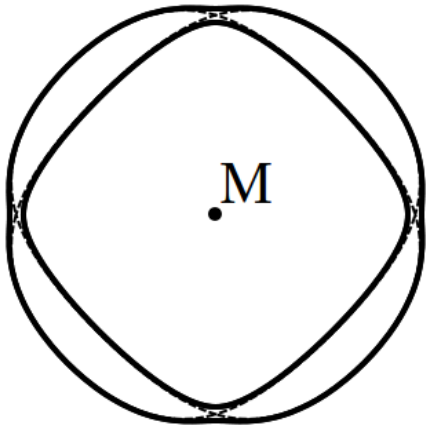

center of inversion

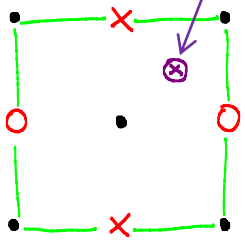

- All states doubly degenerate (Kramers degeneracy)
- The only symmetry allowed 4-fold degeneracy is at the M-point

Spin-density wave order parameters

Collinear SDW order parameter – one of the E_M components condenses

Magnetic moment on iron → the orbital part is E_{M4}

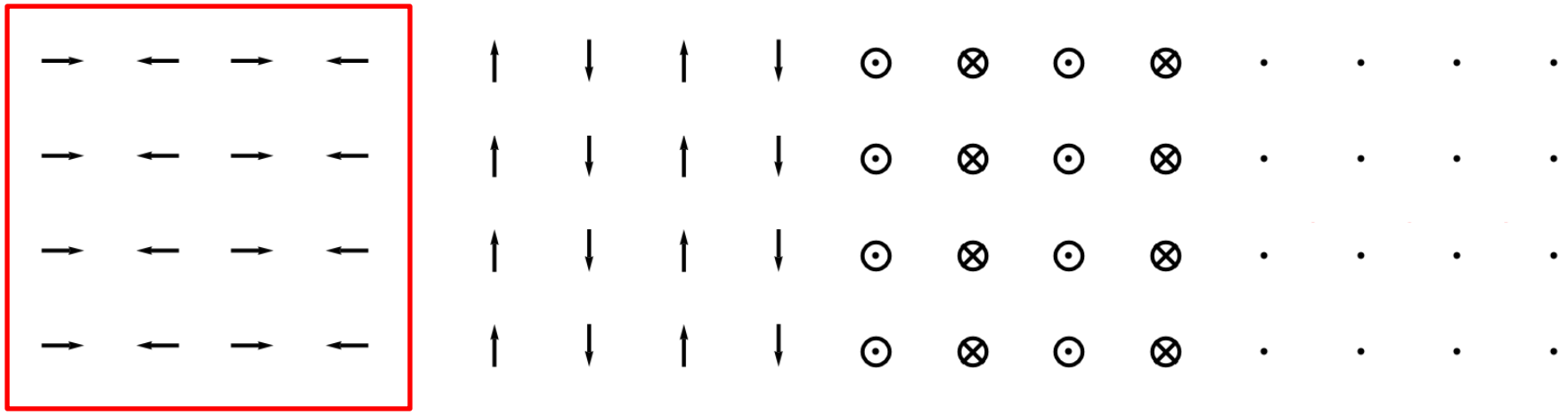

$E_{M1}{}^{Y} = E_{M4}{}^{X} S^{X}$ $E_{M2}{}^{Y} = E_{M4}{}^{X} S^{Y}$ $E_{M3}{}^{X} = E_{M4}{}^{X} S^{z}$ $E_{M4}{}^{X}$

Spin-orbit interaction:

- Magnetic moment locking

Experiments (e.g., 1111 – Qiu et. al. PRL 2008; C. de la Cruz et al., Nature 453, 899 (2008); 122 – Huang et.al. PRL 2008; J. Zhao et al., Nat. Mater. 7, 953 (2008)): the total order parameter is $E_{M4}{}^{X} S^{X} = E_{M1}{}^{Y}$

Induced magnetic moment on pnictogen atoms

Nodal Dirac fermions in the collinear SDW phase

E_{M4} SDW order parameter – symmetry protected Dirac nodes

Y. Ran, *et al.*, Phys. Rev. B **79**, 014505 (2009)

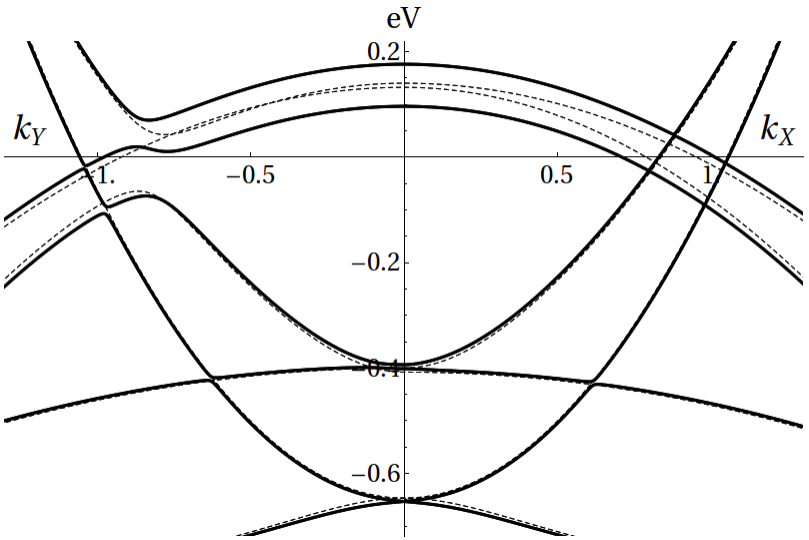

Spin-orbit coupling:

- All the Dirac nodes gapped (gaps ≈ 0.25meV and higher)
- The degeneracies at the M-point lifted by the SDW

The Kramers degeneracy still present (inv. and TR)

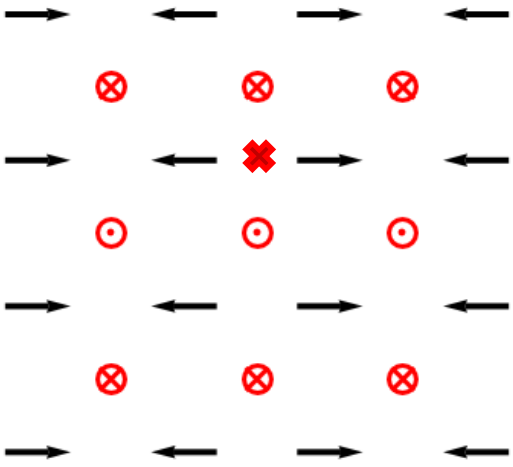

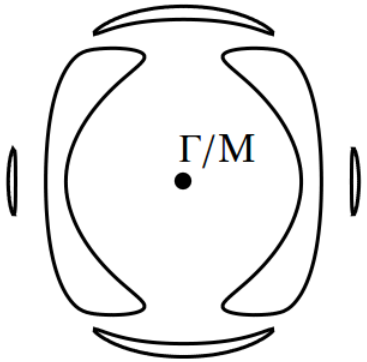

Spin-density wave order parameters

$Ba_{0.76}Na_{0.24}Fe_2As_2$ (S. Avci et.al. Nature Comm. 5, 3845 (2014))

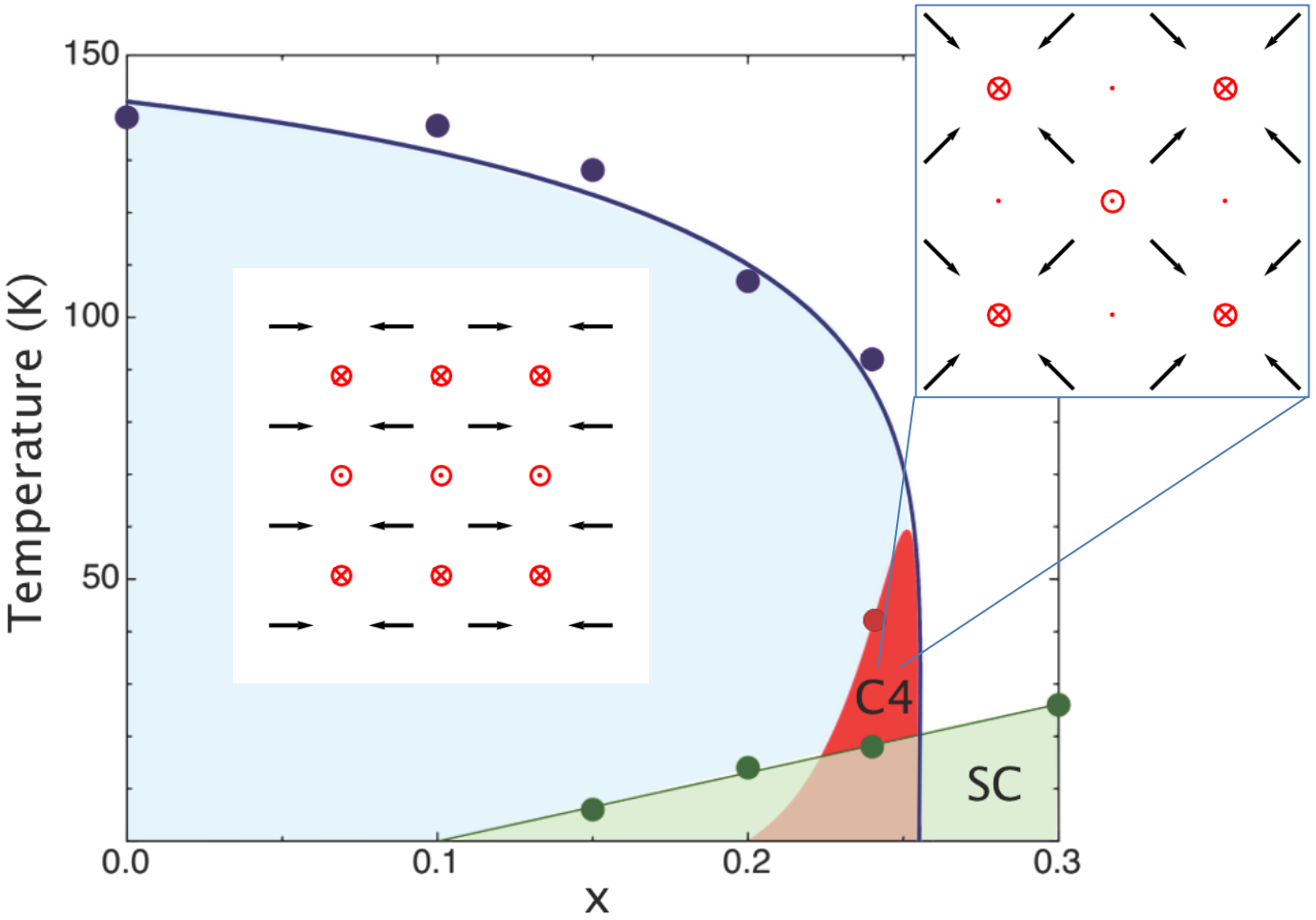

C_4-symmetric phase

The spectrum in the coplanar SDW phase

Coplanar SDW order parameter – both of the E_M components condense

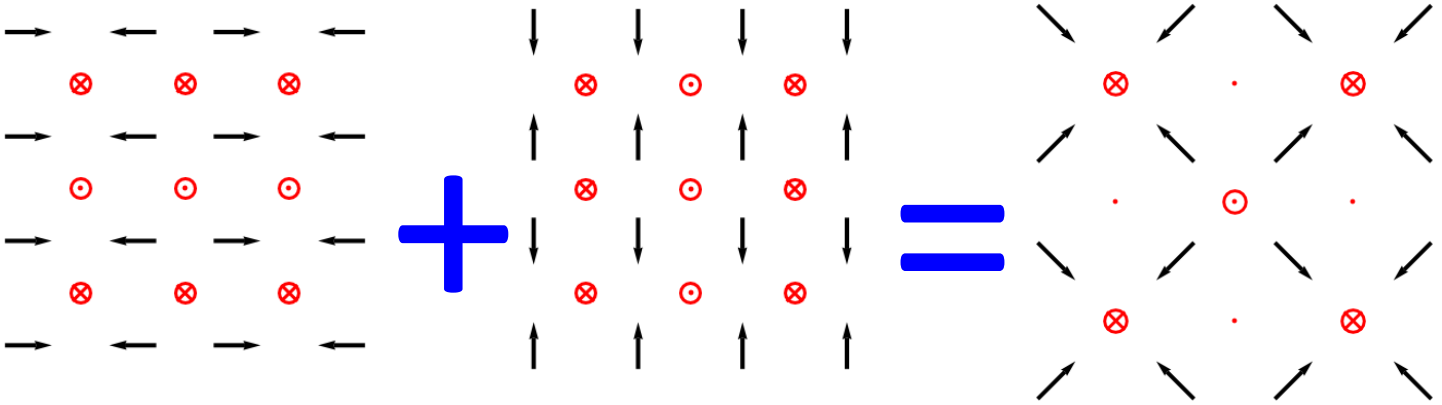

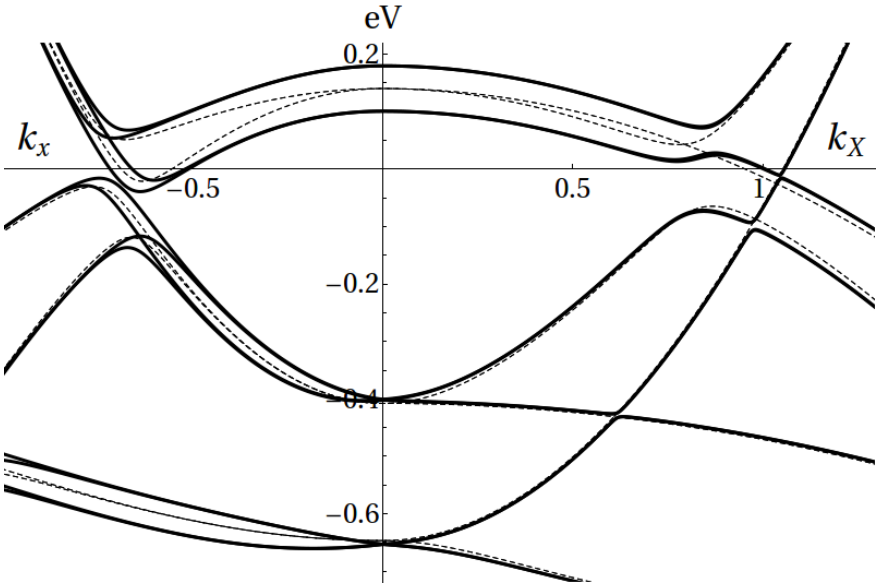

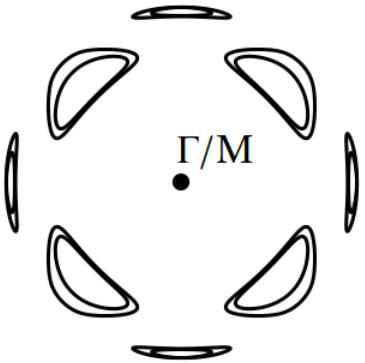

- No Kramers degeneracy
- Fermi surfaces split

Superconductivity

A_{1g} spin-singlet SC specified by three **k**-independent parameters

$$H_{\Gamma,\mathrm{SC}} = \Delta_\Gamma \sum_{\mathbf{k}} \psi^T_{\Gamma,\downarrow}(-\mathbf{k})\,\psi_{\Gamma,\uparrow}(\mathbf{k}) + h.c.$$

$$H_{\mathbf{M},\mathrm{SC}} = \sum_{\mathbf{k}} \sum_{a=X,Y} \psi^T_{a,\downarrow}(-\mathbf{k}) \begin{pmatrix} \Delta_{\mathbf{M}1} & 0 \\ 0 & \Delta_{\mathbf{M}3} \end{pmatrix} \psi_{a,\uparrow}(\mathbf{k}) + h.c.$$

Bogolyubov-de Gennes Hamiltonian

$$H_{\Gamma,\mathrm{BdG}} = \sum_{\mathbf{k}} \Psi_\Gamma(\mathbf{k})^\dagger \begin{pmatrix} h_\Gamma(\mathbf{k}) & \Delta_\Gamma \mathbf{1} \\ \Delta_\Gamma \mathbf{1} & -h_\Gamma(\mathbf{k}) \end{pmatrix} \Psi_\Gamma(\mathbf{k})$$

$$H_{\mathbf{M},\mathrm{BdG}} = \sum_{\mathbf{k}} \Psi_\mathbf{M}(\mathbf{k})^\dagger \begin{pmatrix} h_\mathbf{M}(\mathbf{k}) & \hat{\Delta}^\dagger_\mathbf{M} \\ \hat{\Delta}_\mathbf{M} & -h_\mathbf{M}(\mathbf{k}) \end{pmatrix} \Psi_\mathbf{M}(\mathbf{k})$$

- Hole FS's – the gap is isotropic
- Electron FS's – the gap anisotropy determined by $\Delta_{\mathbf{M}1}$ and $\Delta_{\mathbf{M}3}$

$$\Delta_\mathbf{M} = \begin{pmatrix} \Delta_{\mathbf{M}1} & 0 & 0 & 0 \\ 0 & \Delta_{\mathbf{M}3} & 0 & 0 \\ 0 & 0 & \Delta_{\mathbf{M}1} & 0 \\ 0 & 0 & 0 & \Delta_{\mathbf{M}3} \end{pmatrix}$$

Superconductivity (spin-singlet)

The gap on the electron Fermi surfaces given by

$$\Delta^{(1+)} = \frac{1}{2}(\Delta_{M1} + \Delta_{M3}) + \frac{1}{2}(\Delta_{M1} - \Delta_{M3})\frac{u_-(\mathbf{k})}{-u_+(\mathbf{k})}$$

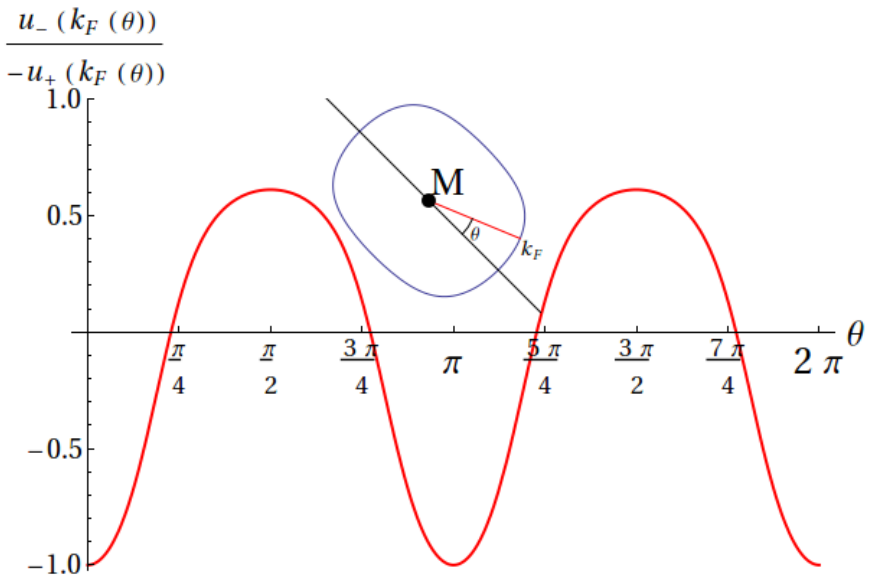

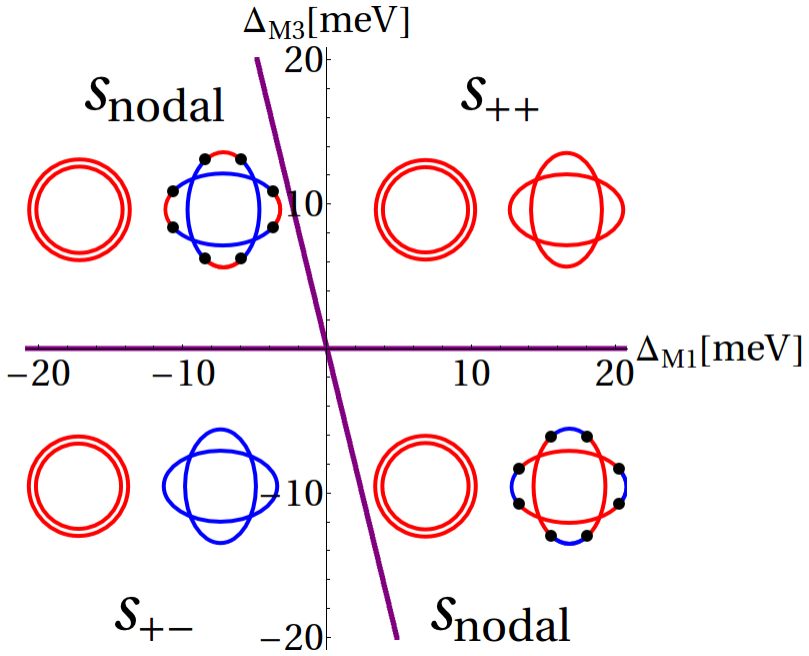

Superconductivity in the presence of spin-orbit coupling

Spin orbit interaction: spin-triplet SC admixture

A_{1g} spin-triplet SC: two more gap parameters

$$H_{\Gamma,\mathrm{triplet}} = \Delta_{\Gamma t} \sum_k \psi^T_{\Gamma,\downarrow}(-\mathbf{k}) \begin{pmatrix} 0 & -i \\ i & 0 \end{pmatrix} \psi_{\Gamma,\uparrow}(\mathbf{k}) + h.c.$$

Bogolyubov-de Gennes Hamiltonian at Γ

$$H_{\Gamma,\mathrm{BdG}} = \sum_{\mathbf{k}} \Psi_\Gamma(\mathbf{k})^\dagger \begin{pmatrix} h_\Gamma(\mathbf{k}) + \frac{1}{2}\lambda_\Gamma \tau_2 & \Delta_\Gamma \mathbf{1} + \Delta_{\Gamma t}\tau_2 \\ \Delta_\Gamma \mathbf{1} + \Delta_{\Gamma t}\tau_2 & -h_\Gamma(\mathbf{k}) - \frac{1}{2}\lambda_\Gamma \tau_2 \end{pmatrix} \Psi_\Gamma(\mathbf{k})$$

The gap on the hole FS's is

$$\Delta_\Gamma^{\mathrm{FS}} = \left| \Delta_\Gamma - \frac{\lambda_\Gamma}{2A_{\mathbf{k}}} \Delta_{\Gamma t} \right| + \ldots$$

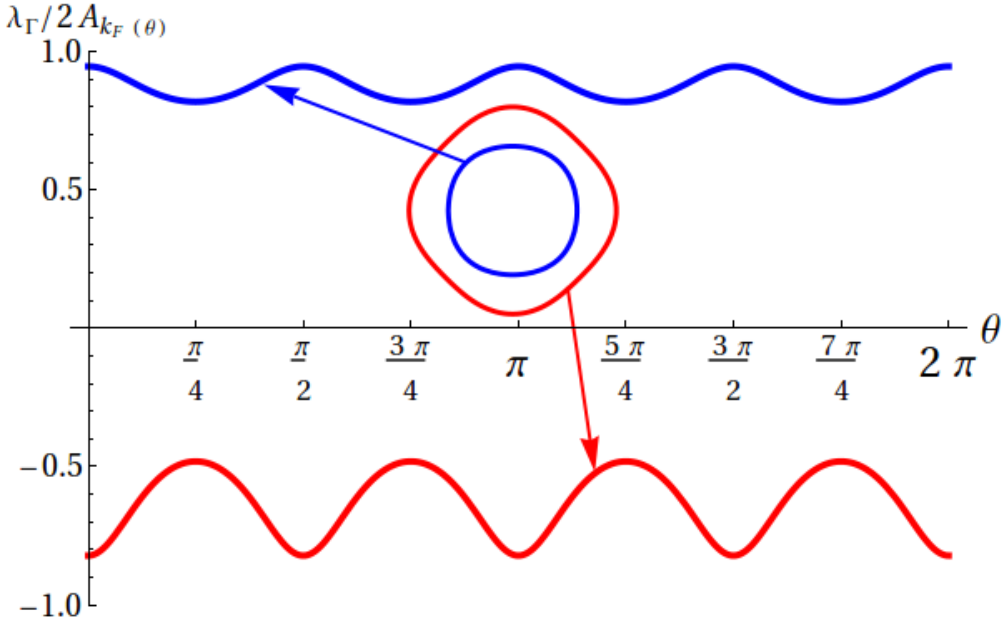

- $\Delta_{\Gamma t}$ → hole FS's gap anisotropy
- ``Near nodes'' in the gap on one FS
- The other FS relatively isotropic

Superconductivity in the presence of spin-orbit coupling

At the M-point:

$$H_{\mathbf{M},\text{triplet}} = \Delta_{\mathbf{M}t} \sum_{\mathbf{k}} \left(\psi^T_{X\downarrow}(-\mathbf{k}) \begin{bmatrix} 0 & -i \\ -1 & 0 \end{bmatrix} \psi_{Y\downarrow}(\mathbf{k}) + \psi^T_{Y\uparrow}(-\mathbf{k}) \begin{bmatrix} 0 & 1 \\ -i & 0 \end{bmatrix} \psi_{X\uparrow}(\mathbf{k}) \right) + h.c.$$

The gap on the electron FS's is

$$\Delta^{\text{FS}}_{\mathbf{M}\pm} = \left| \tfrac{1}{2}(\Delta_{\mathbf{M}1} + \Delta_{\mathbf{M}3}) + \tfrac{1}{2}(\Delta_{\mathbf{M}1} - \Delta_{\mathbf{M}3})\alpha_{\mathbf{M}}(\mathbf{k}) + \Delta_{\mathbf{M}t}\alpha_{\mathbf{M}t}(\mathbf{k}) \right| + \ldots$$

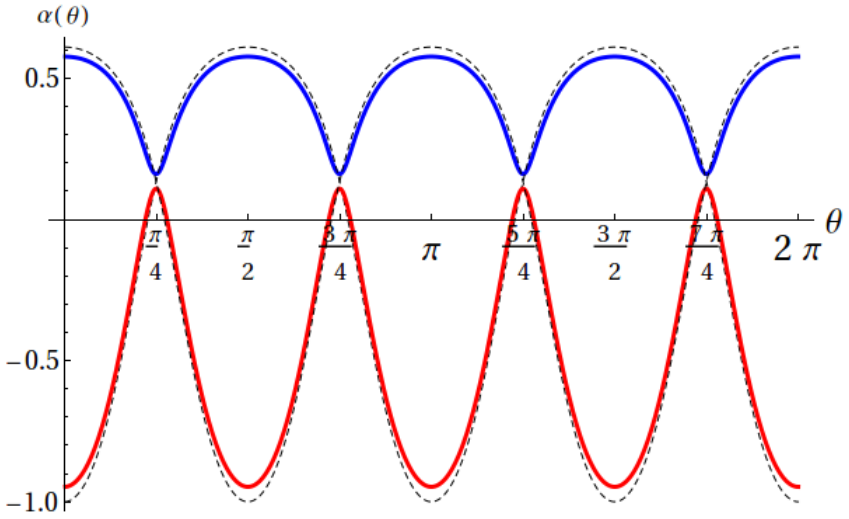

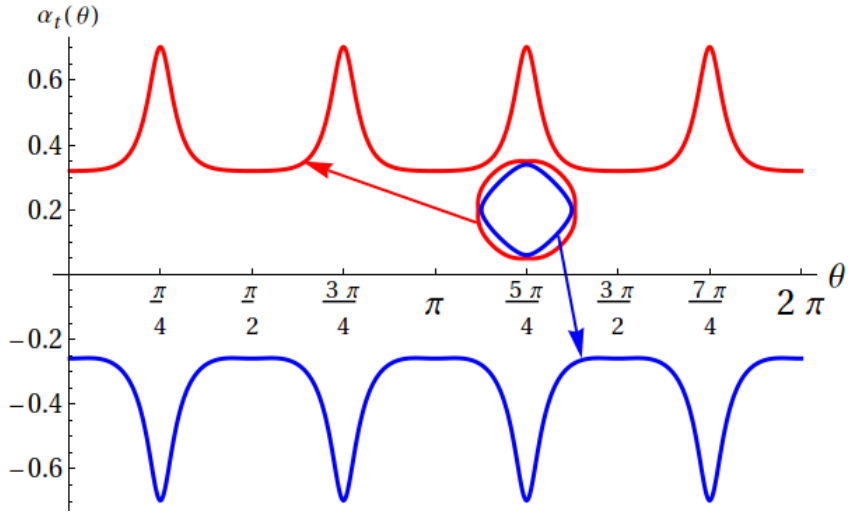

Fourfold gap symmetry

Conclusions

- Used space group symmetry to build the low energy effective model
  - degeneracy at **M**-point
  - spin-orbit interaction is readily included

- Order parameters classified according to the symmetry breaking
  - collinear SDW – a single $E_{\mathbf{M}}$-component (Kramers present)
  - coplanar SDW – both $E_{\mathbf{M}}$-components (Kramers broken)
  - spin-orbit: spin direction locking and induced pnictogen magnetic moment

- A_{1g}-superconductivity (s-wave):
  - spin-singlet: 3 parameters; gap isotropic at Γ, anisotropic at **M**

- A_{1g}-superconductivity (s-wave) with spin-orbit:
  - spin-triplet admixture; 2 parameters; anisotropy and near nodes at Γ, 4-fold gap dependence at M

Future directions

electron-electron interactions:

The interaction Hamiltonian

$$H^{(0)}_{\text{int,dir}} = \frac{1}{2}\int \mathrm{d}\mathbf{r} \sum_{i=1}^{12}\sum_{j=1}^{M_i} g_i^{(j)} \sum_{m=1}^{dim(i)} \left(\sum_{\sigma=\uparrow,\downarrow} \psi^\dagger_\sigma(\mathbf{r}) \Gamma^{(m)}_{i,j} \psi_\sigma(\mathbf{r}) \right)^2$$

$$H^{(0)}_{\text{int,mix}} = \frac{1}{2}\int \mathrm{d}\mathbf{r} \sum_{i=1,4}\sum_{j=1}^{2}\sum_{j'=j+1}^{3} \tilde{g}_i^{(j,j')} \times \left(\sum_{\sigma=\uparrow,\downarrow} \psi^\dagger_\sigma(\mathbf{r}) \Gamma^{(1)}_{i,j} \psi_\sigma(\mathbf{r}) \right) \left(\sum_{\sigma'=\uparrow,\downarrow} \psi^\dagger_{\sigma'}(\mathbf{r}) \Gamma^{(1)}_{i,j'} \psi_{\sigma'}(\mathbf{r}) \right)$$

$$H^{(\mathbf{M})}_{\text{int}} = \frac{1}{2}\int \mathrm{d}\mathbf{r} \sum_{i=13}^{20} g_i \sum_{m=1}^{2} \left(\sum_{\sigma=\uparrow,\downarrow} \psi^\dagger_\sigma(\mathbf{r}) \Gamma^{(m)}_{i,1} \psi_\sigma(\mathbf{r}) \right)^2$$

Where $\Gamma_{i,j}^{(m)}$'s are 6x6 Hermitian matrices

30 independent couplings

Phys. Rev. B **88**, 134510 (2013)

i	I.R.$^{\text{TRS}}$	$\Gamma^{(m)}_{i,1}, \Gamma^{(m)}_{i,2}, \ldots \Gamma^{(m)}_{i,M_i}$
1	A^+_{1g}	$\lambda_\Gamma \mathbb{1}_2, \lambda_{\mathbf{M}} \mathbb{1}_2, \lambda_{\mathbf{M}} \sigma_3$
2	A^-_{1u}	$\lambda_2 \frac{\mathbb{1}_2 - \sigma_3}{\sqrt{2}}$
3	A^-_{2g}	$\lambda_\Gamma \sigma_2$
4	A^+_{2u}	$\lambda_1 \frac{\mathbb{1}_2 + \sigma_3}{\sqrt{2}}$
5	B^+_{1g}	$\lambda_\Gamma \sigma_1$
6	B^-_{1u}	$\lambda_2 \frac{\mathbb{1}_2 + \sigma_3}{\sqrt{2}}$
7	B^+_{2g}	$\lambda_\Gamma \sigma_3, \lambda_3 \mathbb{1}_2, \lambda_3 \sigma_3$
8	B^+_{2u}	$\lambda_1 \frac{\mathbb{1}_2 - \sigma_3}{\sqrt{2}}$
9	E^+_g	$\left(\frac{\lambda_1 \sigma_1 + \lambda_2 \sigma_2}{\sqrt{2}}, \frac{-\lambda_1 \sigma_1 + \lambda_2 \sigma_2}{\sqrt{2}} \right)$
10	E^+_u	$\left(\frac{-\lambda_3 + \lambda_{\mathbf{M}}}{\sqrt{2}} \sigma_1, \frac{\lambda_3 + \lambda_{\mathbf{M}}}{\sqrt{2}} \sigma_1 \right)$
11	E^-_g	$\left(\frac{-\lambda_1 \sigma_2 + \lambda_2 \sigma_1}{\sqrt{2}}, \frac{\lambda_1 \sigma_2 + \lambda_2 \sigma_1}{\sqrt{2}} \right)$
12	E^-_u	$\left(\frac{-\lambda_3 + \lambda_{\mathbf{M}}}{\sqrt{2}} \sigma_2, \frac{\lambda_3 + \lambda_{\mathbf{M}}}{\sqrt{2}} \sigma_2 \right)$
13	$E^+_{\mathbf{M}1}$	$\left(\lambda_4 \frac{\mathbb{1}_2 - \sigma_3}{\sqrt{2}}, \frac{\lambda_6 \sigma_1 + \lambda_7 \sigma_2}{\sqrt{2}} \right)$
14	$E^-_{\mathbf{M}1}$	$\left(\lambda_5 \frac{\mathbb{1}_2 - \sigma_3}{\sqrt{2}}, \frac{-\lambda_6 \sigma_2 + \lambda_7 \sigma_1}{\sqrt{2}} \right)$
15	$E^+_{\mathbf{M}2}$	$\left(\frac{\lambda_4 \sigma_1 + \lambda_5 \sigma_2}{\sqrt{2}}, \lambda_6 \frac{\mathbb{1}_2 - \sigma_3}{\sqrt{2}} \right)$
16	$E^-_{\mathbf{M}2}$	$\left(\frac{-\lambda_4 \sigma_2 + \lambda_5 \sigma_1}{\sqrt{2}}, \lambda_7 \frac{\mathbb{1}_2 - \sigma_3}{\sqrt{2}} \right)$
17	$E^+_{\mathbf{M}3}$	$\left(\lambda_4 \frac{\mathbb{1}_2 + \sigma_3}{\sqrt{2}}, \frac{\lambda_6 \sigma_1 - \lambda_7 \sigma_2}{\sqrt{2}} \right)$
18	$E^-_{\mathbf{M}3}$	$\left(\lambda_5 \frac{\mathbb{1}_2 + \sigma_3}{\sqrt{2}}, \frac{\lambda_6 \sigma_2 + \lambda_7 \sigma_1}{\sqrt{2}} \right)$
19	$E^+_{\mathbf{M}4}$	$\left(\frac{\lambda_4 \sigma_1 - \lambda_5 \sigma_2}{\sqrt{2}}, \lambda_6 \frac{\mathbb{1}_2 + \sigma_3}{\sqrt{2}} \right)$
20	$E^-_{\mathbf{M}4}$	$\left(\frac{\lambda_4 \sigma_2 + \lambda_5 \sigma_1}{\sqrt{2}}, \lambda_7 \frac{\mathbb{1}_2 + \sigma_3}{\sqrt{2}} \right)$

Space group P4/nmm

Operations:

Integer lattice translations $\mathbb{T} = \{\{e|\mathbf{t}\}|\ \mathbf{t} = m_1\mathbf{a}_1 + m_2\mathbf{a}_2 + m_3\mathbf{a}_3\}$

`Point group', i.e., symmetries of the unit cell:

$\mathbf{D}_{4h}$

Generators:

$\{\sigma^X|\frac{1}{2}\frac{1}{2}\}$

$\{\sigma^x|00\}$

$\{\sigma^z|\frac{1}{2}\frac{1}{2}\}$

P4/nmm is non-symmorphic